Unimolecular Pyrolysis Mechanisms of Monothioformic and Dithioformic Acids. An ab Initio Study and Evaluation of Rate Constant

Jian-Hua Huang, Ke-Li Han,* Rong-Shun Zhu, Guo-Zhong He, and Nan-Quan Lou

State Key Laboratory of Molecular Reaction Dynamics, Dalian Institute of Chemical Physics, Chinese Academy of Sciences, Dalian 116023, China

Received: October 1, 1997; In Final Form: December 17, 1997

Calculations at both the SCF and MP2 levels including electron correlation effects on both the geometries and energies of different stationary points encountered along the decomposition pathways for thioformic acids are reported. Four conformers of monothioformic acid and two conformers of dithioformic acids have been investigated using ab initio electronic structure calculations with a series of basis sets. Results show that the *keto* tautomer of monothioformic acid, HC(:O)SH, is the more stable form with respect to the *thioketo* tautomer, HC(:S)OH. Furthermore, all of the *trans* isomers of monothioformic and dithioformic acids are slightly more stable in energy than the corresponding *cis* isomers, which are in agreement with experimental results. Rice−Ramsperger−Kassel−Marcus (RRKM) calculations of the unimolecular rate constants for pyrolysis of these acids are carried out.

Introduction

Recently, there has been considerable interest in the study of sulfur-containing organic compounds because of their importance in chemistry and in biology.[1] The structures of monothioformic acid have been assigned by microwave spectroscopy.[2] Monothioformic acid exhibits structural, as well as geometric, isomerism, with the *keto* and *thioketo* forms HC(:O)SH and HC(:S)OH. Engler and Gattow[3] suggested that the *keto* tautomer is the more stable form. Hocking and co-workers confirmed this suggestion and also indicated that the *keto* tautomer displayed *cis*−*trans* isomerism, with the *trans* conformer being more stable by 231 cm^{-1} (0.661 kcal/mol).[4] The microwave spectrum of dithioformic acids (HCSSH), as a potential interstellar molecule has been studied by Bak and coworkers.[5,6] Their results showed that the *trans* isomer was stabilized relative to the *cis* isomer by 350 cm^{-1} (1.002 kcal/mol). Previously, ab initio studies on the properties of monothioformic and dithioformic acids, including the structural information, rotation isomerization, electronic properties, intramolecular hydrogen bond, and hydrogen shift reaction, etc., were also reported.[7−15] Calculations by So[8] showed that the *trans* isomer of dithioformic acid was more stable than its *cis* isomer by 696 cm^{-1} (1.992 kcal/mol) at the MP2/3-21G*//HF/3-21G* level, whereas Ioannoni et al.[10] found the *trans* isomer to be more stable by 1.37 kcal/mol at the MP4SDTQ//HF/6-31G* level. Nguyen and Weringa[14] studied a 1,3-hydrogen shift in thioformic acid and gave an energy difference of 2.95 kcal/mol at the MP4SDTQ/6-31G*//HF/6-31G* level between the two isomers of monothioformic acid, with the trans-HC(:O)SH being more stable than the *trans*-HC(:S)OH. All of the above experimental and theoretical studies, however, were more concerned with the molecular structures and properties of thioformic acids. Only very recently did Xie et al.[16] report the theoretical studies of unimolecular pyrolysis of dithioformic acid. They investigated pyrolysis of dithioformic acids using the SCF MO method at the MP4/6-31G**//HF/6-31G** level, but for pyrolysis of monothioformic acid no papers have been reported as yet.

In this work, we explore the possible mechanisms of unimolecular pyrolysis reactions of monothioformic and dithioformic acids in the absence of experimental data. Similar to Ruelle et al.'s studies on pyrolysis mechanisms of formic acid,[17] we propose that the following thermal decomposition reactions occur during the pyrolysis of monothioformic and dithioformic acids.

keto conformers of monothioformic acid:

$$\textit{trans}\text{-HC(:O)SH} \rightarrow H_2S + CO \quad (1)$$

$$\textit{cis}\text{-HC(:O)SH} \rightarrow H_2 + SCO \quad (2)$$

thioketo conformers of monothioformic acid:

$$\textit{trans}\text{-HC(:S)OH} \rightarrow H_2O + CS \quad (3)$$

$$\textit{cis}\text{-HC(:S)OH} \rightarrow H_2 + OCS \quad (4)$$

dithioformic acid:

$$\textit{trans}\text{-HCSSH} \rightarrow H_2S + CS \quad (5)$$

$$\textit{cis}\text{-HCSSH} \rightarrow H_2 + SCS \quad (6)$$

All the structures and energies of the stationary points and the transition states involved in these reactions are examined using ab initio methods. Effects of basis sets involving polarization function and diffuse function as used by Császár,[18] as well as electron correlation upon the relative stability of these structures and reaction heats for each of the above reactions, are compared and discussed. Moreover, the reactivities for the three pairs of competing reactions are expected to be predicted by means of the RRKM rate constant calculations using the UNIMOL program.

Computational Procedure

All molecular structures, including those for transition states in the reactions considered here, were determined by the search

* Author to whom correspondence should be addressed.

S1089-5639(97)03213-1 CCC: $15.00
Published on Web 02/24/1998

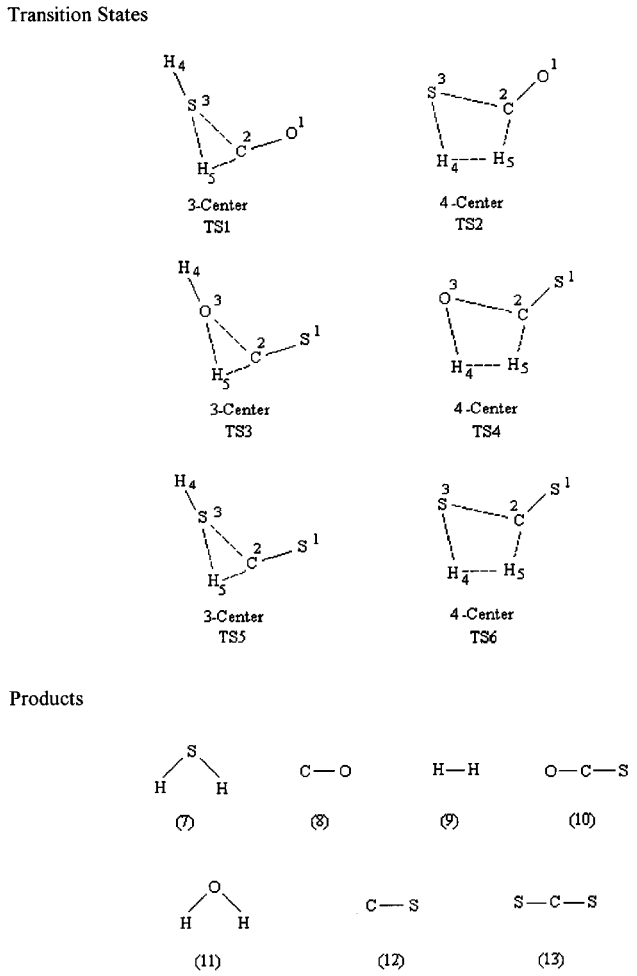

Figure 1. Optimized geometries of the stationary points that are relevant in the thioformic acid pyrolysis.

methods in GAUSSIAN 94W.[19] These geometries were fully optimized with a variety of basis sets (6-31G*, 6-311G**) and include large basis sets involving diffuse functions (6-311++G**) at the SCF level, as well as at the MP2 level considering electron correlation with 6-31G*, 6-311G**, and 6-311++G** basis sets. Harmonic vibrational frequencies were calculated, at both the MP2/6-311G** and MP2/6-311++G** levels with their corresponding structures, to characterize the stationary points and to estimate the zero-point vibrational contributions to relative energies. To obtain improved energy, at each of the final MP2/6-311G** structures, as well as at the MP2/6-311++G** structures, single-point energy calculations were carried out with fourth-order Møller−Plesset perturbation theory,[20,21] denoted as MP4SDTQ/6-311G**//MP2/6-311G** and MP4SDTQ/6-311++G**//MP2/6-31++G**. For some saddle points, the intrinsic reaction coordinate (IRC)[22] calculations were performed in order to establish which two stable points were connected.

Results and Discussion

A. Optimized Structures and Energetics. Geometrical parameters for all of the species encountered on the pyrolysis of monothioformic and dithioformic acids optimized at both the SCF and MP2 levels with a series of basis sets are given in Figure 1 and Table 1. All these structures are found to be planar.

Considering first the geometries of the equilibrium structure, it can easily be observed that, at every level of theory, both lengths are generally decreased when polarization function and diffuse function are added to the atomic basis set. On the other hand, as shown by DeFrees et al.,[23] the correlation corrections result always in bond lengthening for each of the basis sets used. Relative to the HF/6-31G* and HF/6-311G** values, the MP2/6-31G* and MP2/6-311G** bond lengths of equilibrium structures can be regarded as resulting from the lengthening by inclusion of the MP2 correction, respectively. But compared with HF/6-31G* values, the MP2/6-311G** bond lengths of equilibrium structures can be regarded as resulting from the two opposing but not equal effects: shortening of the bond lengths by extension of the basis set and lengthening by inclusion of the MP2 corrections. As for the transition state structures (TS1−TS6), the effects of the basis set extension are found to have trends similar to those mentioned for the equilibrium structures (shortening the bond length), but the correlation effect does not operate always in the same direction for all geometrical parameters. For instance, the C2−S3 bond lengths in TS1 are 2.52, 2.514 Å at the HF/6-31G* and HF/6-311G* levels, respectively, but they are 2.428, 2.376 Å at the MP2/6-31G* and MP2/6-311G** levels. In our calculations, as shown in Table 1, the geometrical differences between the two highest levels of MP2/6-311G** and MP2/6-311++G** are very slight. Generally, basis sets with diffuse functions are important for anions and systems where electrons are relatively far from the nucleus and systems with significant negative charge.[19]

Table 2 displays the relative energies including the zero-point energy corrections for the conformers and transition states involved in pyrolysis of thioformic acids. The relative stability of those conformers is dependent upon basis sets and inclusion of correlation effects. It is easily seen that, for all the *trans*−*cis* conformers, the *trans* conformers are the more stable structures. Moreover, for the monothioformic acid, the *keto* tautomer of monothioformic acid HC(:O)SH is more stable than the corresponding *thioketo* tautomer HC(:S)OH, which is agrees well with both experimental and theoretical results.[3,4,14] Because of the relatively larger basis sets and relatively higher optimization level used here, the energy difference in our calculation is closer to the experimental results than other calculations. For example, in our calculation, the *trans*-HC(:O)SH (**1**) is more

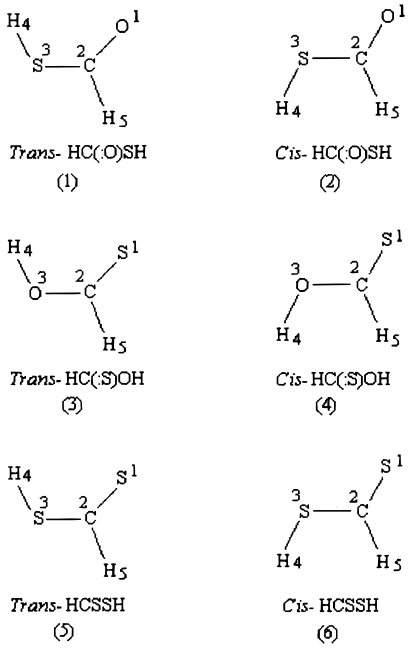

stable than *cis*-HC(:O)SH (**2**) by 1.08 kcal/mol at the MP4SDTQ/6-311G**//MP2/6-311G** level; the value obtained experi-

TABLE 1: Optimized Structures of the Stationary Points for the Thioformic Acid Decomposition (Bond Lengths, Å; Bond Angles, deg)

structure	param	MP2/ 6-311G**	MP2/ 6-311++G**	structure	param	MP2/ 6-311G**	MP2/ 6-311++G**
trans-HC(:O)SH (**1**)	O1−C2	1.206	1.209	four-center	O1−C2	1.178	1.181
	C2−S3	1.777	1.770	transition state TS2	C2−S3	1.677	1.674
	S3−H4	1.336	1.337		S3−H4	1.691	1.698
	C2−H5	1.105	1.104		C2−H5	1.436	1.429
	O1−C2−S3	125.4	125.8		H4−H5	0.998	0.993
	C2−S3−H4	93.5	94.1		O1−C2−S3	145.6	145.4
	O1−C2−H5	123.6	123.2		C2−S3−H4	55.9	55.5
	H4−S3−C2−O1	0.0	0.0		S3−H4−H5	124.7	124.7
cis-HC(:O)SH (**2**)	O1−C2	1.205	1.207		H4−S3−C2−O1	180.0	180.0
	C2−S3	1.779	1.774	three-center	S1−C2	1.536	1.524
	S3−H4	1.335	1.336	transition state TS3	C2−O3	1.934	2.041
	C2−H5	1.106	1.105		O3−H4	0.967	0.968
	O1−C2−S3	122.8	123.0		C2−H5	1.203	1.161
	C2−S3−H4	94.7	94.5		O3−H5	1.271	1.364
	O1−C2−H5	123.5	123.2		S1−C2−O3	131.5	134.2
	H4−S3−C2−O1	180.0	180.0		C2−O3−H4	157.8	161.1
trans-HC(:S)O (**3**)	S1−C2	1.618	1.616		C2−H4−H5	37.3	32.8
	C2−O3	1.337	1.341		H4−O3−C2−S1	0.0	0.0
	O3−H4	0.969	0.970	four-center	S1−C2	1.586	1.585
	C2−H5	1.091	1.089	transition state TS4	C2−O3	1.265	1.269
	S1−C2−O3	126.7	126.5		O3−H4	1.326	1.337
	C2−O3−H4	106.3	106.8		C2−H5	1.400	1.389
	S1−C2−H5	123.7	123.8		H4−H5	0.999	0.998
	H4−O3−C2−S1	0.0	0.0		S1−C2−O3	145.7	145.1
cis-HC(:S)OH (**4**)	S1−C2	1.612	1.609		C2−O3−H4	65.2	64.7
	C2−O3	1.346	1.351		O3−H4−H5	124.5	123.9
	O3−H4	0.964	0.965		H4−O3−C2−S1	180.0	180.0
	C2−H5	1.095	1.094	three-center	S1−C2	1.541	1.541
	S1−C2−O3	123.6	123.3	transition state TS5	C2−S3	2.548	2.538
	C2−O3−H4	107.8	108.4		S3−H4	1.342	1.342
	S1−C2−H5	122.4	122.8		C2−H5	1.106	1.106
	H4−O3−C2−S1	180.0	180.0		S3−H5	1.929	1.929
trans-HCSSH (**5**)	S1−C2	1.622	1.621		S1−C2−S3	113.7	113.6
	C2−S3	1.738	1.738		C2−S3−H4	100.6	101.0
	S3−H4	1.338	1.337		C2−S3−H5	23.9	24.1
	C2−H5	1.092	1.092		H4−S3−C2−S1	180.0	180.0
	S1−C2−S3	128.7	128.7	four-center	S1−C2	1.604	1.603
	C2−S3−H4	95.6	95.5	transition state TS6	C2−S3	1.669	1.670
	S1−C2−H5	121.2	121.2		S3−H4	1.772	1.771
	H4−S3−C2−S1	0.0	0.0		C2−H5	1.343	1.343
cis-HCSSH (**6**)	S1−C2	1.620	1.620		H4−H5	0.943	0.944
	C2−S3	1.744	1.745		S1−C2−S3	143.8	143.9
	S3−H4	1.337	1.337		C2−S3−H4	48.9	48.9
	C2−H5	1.091	1.092		S3−H4−H5	127.2	127.1
	S1−C2−S3	124.5	124.5		H4−S3−C2−S1	180.0	180.0
	C2−S3−H4	96.1	96.1	H_2S (**7**)	S−H	1.334	1.333
	S1−C2−H5	121.6	121.6		H−S−H	92.2	92.1
	H4−S3−C2−S1	180.0	180.0	CO (**8**)	C−O	1.139	1.140
three-center	O1−C2	1.142	1.143	H_2 (**9**)	H−H	0.738	0.738
transition state TS1	C2−S3	2.376	2.370	OCS (**10**)	O−C	1.169	1.171
	S3−H4	1.335	1.334		C−S	1.565	1.563
	C2−H5	1.202	1.208		O−C−S	180.0	180.0
	S3−H5	1.748	1.739	H_2O (**11**)	O−H	0.958	0.959
	O1−C2−S3	146.9	148.1		H−O−H	102.5	103.5
	C2−S3−H4	173.9	173.9	CS (**12**)	C−S	1.542	1.540
	C2−S3−H5	29.1	29.4	CS_2 (**13**)	S−C	1.562	1.562
	H4−S3−C2−O1	0.0	0.0		S−C−S	180.0	180.0

mentally by Hocking and Winnewisser[4] is 231 cm^{-1} (0.661 kcal/mol), whereas it is 2.95 kcal/mol in Nguyen Weringa's calculation at the MP4/6-31G**//HF/6-31G** level,[14] and they overestimated it by 2.289 kcal/mol. Moreover, the *trans*-HCSSH is more stable than the *cis*-HCSSH by 1.25 kcal/mol at the MP4SDTQ/6-311G**//MP2/6-311G** level in our calculations; the experimental result[5,6] is 350 cm^{-1} (1.002 kcal/mol), whereas calculations by So,[8] by Ioannoni et al.,[10] and by Xie and co-workers[16] give the values of 1.992, 1.37, and 1.55 kcal/mol, at the MP2/3-21G*//HF/3-21G*, MP4SDTQ/6-31G*//HF/6-31G*, and MP4/6-31G**//HF/6-31G** levels, respectively.

B. Pyrolysis of Thioformic Acid. Considering first reactions 1 and 2 corresponding to decomposition of the two isomers of *keto*-HC(:O)SH. The concerted mechanism of dehydrogensulfidation of *trans*-HC(:O)SH (**1**) is assumed as a 1,2-shift of the H5 atom to the S3 atom of the SH hydrosulfide group via a three-center transition state TS1 in which the formation of the S3−H5 bond and the breaking of the C2−H5 and C2−S3 bonds take place simultaneously. However, the variation of these bond lengths in the transition state with respect to their equilibrium values in *trans*-HC(:O)SH is apparent; the breaking bonds, both C2−H5 and C2−S3, are elongated, but the S3−H5 bond length is shortened, and the differences among various

TABLE 2: Relative Energies (kcal/mol) Plus Zero-Point Energy at Different Levels for Pyrolysis of Monothioformic and Dithioformic Acids

rel energy	HF/6-31G*// HF/6-31G*	HF/6-311G**// HF/6-311G**	MP4SDTQ/6-311G**// MP2/6-311G**	MP4SDTQ/6-311+G**// MP2/6-311+G**
		Relative Energies Involving Pyrolysis of Monothioformic Acid		
ΔE[a](**2**−**1**)	1.42	1.11	1.08, 0.661[c]	1.09, 2.95[d]
ΔE(**3**−**1**)	5.47	4.88	5.41	5.72
ΔE(**4**−**3**)	6.19	5.98	5.27	4.58
ΔE(TS1−**1**)	67.88	62.83	57.47	59.69
ΔE(TS2−**2**)	90.09	83.20	62.65	63.48
ΔE(TS3−**3**)	109.69	103.72	82.66	74.05
ΔE(TS4−**4**)	92.33	91.97	65.04	65.13
ΔH1[b]	−13.83	−18.42	−10.28	−7.52
ΔH2	−4.74	−4.10	−11.99	−10.62
ΔH3	39.96	34.55	31.45	27.24
ΔH4	−14.97	−13.86	−21.59	−19.84
		Relative Energies Involving Pyrolysis of Dithioformic Acid		
ΔE(**6**−**5**)	1.64	1.39	1.25, 1.002[e]	1.31, 1.55,[f] 1.99,[g] 1.37[h]
ΔE(TS5−**5**)	80.18	75.87	58.78	58.29, 63.68[f]
ΔE(TS6−**6**)	92.28	88.26	68.91	68.58, 72.73[f]
ΔH5	29.72	88.47	27.79	27.08, 29.89[f]
ΔH6	2.61	68.91	−8.58	−8.44, −10.12[f]

[a] ΔE(**2**−**1**) equals the energy of structure **2** minus the energy of structure **1**, and so on. [b] ΔH1 means reaction heat of reaction 1, and so on. [c] Experimentally from ref 4. [d] By Nguyen and Weringa from ref 14 at the MP4SDTQ/6-31G**//HF/6-31G** level. [e] Experimentally from ref 5. [f] By Xie et al. from ref 16 at the MP4/6-31G**//HF/6-31G** level. [g] By So from ref 8 at the MP2/3-21G*//HF/3-21G* level. [h] By Ioannoni et al. from ref 10 at the MP4SDTQ/6-31G*//HF/6-31G* level.

levels for the variation of these bond lengths is very small. The basic trend is that the more elongated the C2−H5 bond is, the less the increase of the C2−S3 bond and the more the decrease of the S3−H5 bond will be.

The mechanism of dehydrogenation yielding H_2 and OCS assumes at first a conformational change from the most stable *trans*-HC(:O)SH (**1**) to the less stable *cis*-HC(:O)SH (**2**). The rotation barrier height is 32.5 kcal/mol.[14] From the *cis* intermediate, the dehydrogenation proceeds via a four-membered transition state TS2 by simultaneous C2−H5 and S3−H4 bond cleavages and H4−H5 bond formation. In contrast to the previous dehydrogensulfidation process, the overall transition state structures are similar in all computational levels. In TS2, the C2−H5 and S3−H4 bond lengths are much more elongated than the corresponding normal bond lengths in *cis*-HC(:O)SH (**2**), whereas the distance between H4 and H5 is closing to the H−H bond length in H_2. To verify which two stable points connect to the transition state, the RHF/6-31G* IRC for reactions 2 and 3 via TS2 (four-membered transition state) and TS3 (three-center transition state) along the reaction path are performed. In the forward direction along the reaction coordinate, the cleaving bonds C2−H5 and C2−S3 in TS3 and C2−H5 and S3−H4 in TS2 are elongated, while the forming S3−H5 bond in TS3 and H4−H5 bond in TS2 become closer to the S−H bond length in H_2S and the H−H bond length in H_2, respectively; the transition states are connected to the products. On the contrary, transition states are connected to the reactants in the reverse direction.

More important than the actual correlation-induced changes in geometry is the effect of those changes on the relative energies of different species encountered on the reaction pathways. For either process, the activation barrier is generally decreased with the basis set increases; furthermore, the barrier heights can be decreased greatly by the correlation effects. A decrease of barrier height for the dehydrogenation process, for instance, as large as 27.44 kcal/mol is obtained in going from HF/6-31G*//HF/6-31G* to MP4SDTQ/6-311G**//MP2/6-311G** calculations. The activation barriers of reactions 1 and 2 corresponding to the dehydrogensulfidation and dehydrogenation processes of *keto*-HC(:O)SH are 57.47 and 62.65 kcal/mol, respectively, at the MP4SDTQ/6-311G**//MP2/6-311G** level, which means dehydrogensulfidation process is the more favorable process in energy than the dehydrogenation process. The reaction heats are −10.28 and −11.99 kcal/mol, respectively.

For reactions 3−6, both reactions 3 and 5 are similar to reaction 1 via three-center transition states (TS3, TS5); they correspond to dehydration and dehydrogensulfidation of *trans*-HC(:O)SH (**3**) and *trans*-HCSSH (**5**), respectively. As well as reactions 4 and 6 resemble reaction 2 via four-membered transition states (TS4, TS6), they correspond to dehydrogenation of *cis*-HC(:O)SH (**4**) and *cis*-HCSSH (**6**), respectively. As seen from the computational results, the geometries including equilibrium structures and transition states involved in these reactions are similar to those in reactions 1 and 2. The effects of basis sets and electronic correlation on the geometries and energy barrier are fundamentally the same as the former discussion. However, there is the unusual fact that, in TS5, the dihedral angle H4−S3−C2−S1 is 0.0° at the STO-3G level, while it is 180.0° at other calculation levels. The activation barriers for reactions 3 and 4 are 82.66, 65.04 kcal/mol and the reaction heats are 31.45, −21.59 kcal/mol at the MP4SDTQ/6-311G**//MP2/6-311G** level, respectively. The activation barriers for reaction 5 and 6 are 58.78, 68.91 kcal/mol and the reaction heats are 27.79, −8.58 kcal/mol at the MP4SDTQ/6-311G**//MP2/6-311G** level, respectively.

It should be noticed that the activation barrier of reaction 5 corresponding to dehydrogensulfidation of HCSSH via a three-center transition state TS5 is lower than the barrier for reaction 6 corresponding to dehydrogenation of HCSSH via a four-membered transition state TS6, which means that the dehydrogensulfidation process is the more favorable process than dehydrogenation in energy for HCSSH, which is in agreement with that of *keto*-HC(:O)SH. However, for the decomposition of *thioketo*-HC(:S)OH, the opposite result is obtained; the activation barrier of dehydration process proceeding from the three-center transition state TS3 is higher than that of the dehydrogenation process via the four-membered transition state TS4, which means the dehydrogenation process is the favorable process. This is perhaps because the cleaving of the C−O bond

TABLE 3: Total Energies (hartrees) at Different Levels of the Stationary Points for Thioformic Acid Decomposition

molecule	ZPE	HF/6-311G**// HF/6-311G**	HF/6-311G**// MP2/6-311G**	HF/6-311++G**// MP2/6-311++G**	MP4SDTQ/6-311G**// MP2/6-311G**	MP4SDTQ/6-311++G**// MP2/6-311++G**
trans-HC(:O)SH (**1**)	17.89	−511.449 325	−511.447 0538	−511.451 8479	−511.960 987	−511.970 1669
cis-HC(:O)SH (**2**)	17.81	−511.447 430	−511.445 2614	−511.450 0308	−511.959 1258	−511.968 3098
trans-HC(:S)OH (**3**)	20.29	−511.445 375	−511.443 5725	−511.447 5195	−511.956 1823	−511.964 6409
cis-HC(:S)OH (**4**)	19.94	−511.435 276	−511.433 5233	−511.438 0817	−511.947 215	−511.956 8156
trans-HCSSH (**5**)	16.78	−834.086 649	−834.086 1869	−834.088 4087	−834.545 4798	−834.550 017
cis-HCSSH (**6**)	16.63	−834.084 197	−834.083 7969	−834.085 8865	−834.543 2488	−834.547 6645
TS1	12.34	−511.340 307	−511.331 624	−511.333 6382	−511.860 5218	−511.865 9975
TS2	12.94	−511.307 031	−511.303 5845	−511.307 6709	−511.851 4826	−511.859 1474
TS3	13.43	−511.269 079	−511.267 8578	−511.281 6263	−511.813 4626	−511.836 2535
TS4	13.60	−511.287 053	−511.284 4618	−511.289 4946	−511.833 4204	−511.842 9149
TS5	12.46	−833.958 810	−833.955 7975	−833.958 8349	−834.444 8872	−834.450 2357
TS6	11.17	−833.934 784	−833.934 0467	−833.936 4551	−834.424 6818	−834.429 4816
H_2S (**7**)	9.83	−398.701 236	−398.701 1073	−398.701 963	−398.870 8828	−398.872 0479
CO (**8**)	3.05	−112.769 475	−112.766 5094	−112.767 9655	−113.098 5045	−113.102 2052
H_2 (**9**)	6.48	−1.132 491	−1.132 4851	−1.132 4864	−1.167 7293	−1.167 7276
OCS (**10**)	5.78	−510.312 632	−510.308 3129	−510.312 6583	−510.801 6611	−510.808 6127
H_2O (**11**)	13.71	−76.047 012	−76.046 2662	−76.052 4781	−76.276 3381	−76.287 3344
CS (**12**)	1.88	−435.335 7922	−435.335 0381	−435.337 6491	−435.622 2077	−435.626 8039
CS_2 (**13**)	4.40	−832.936 4339	−832.935 6469	−832.938 3876	−833.380 0336	−833.384 2807

is more difficult than the cleaving of the C−S bond due to the well-known fact of the C−O bond energy being larger than the C−S bond.

C. Rate Constants Calculations using RRKM Theory. The rate constants were calculated using Rice−Ramsperger−Kassel−Marcus (RRKM) theory. We followed the procedures described by Gilbert and Smith.[24] In the RRKM calculation, the reactants and the transition states were treated as symmetric top with the largest moments of inertia taken to be active. The master equations[25,26] were solved by numerical method, and the density of states for the reactant and TS were calculated using the Beyer−Swinehart algorithm. The Lennard-Jones collision rate between thioformic acids and bath gas Ar was estimated by means of the effective Lennard-Jones diameters and well depths, which were obtained using the multidimensional mid-ordinate rule integration by program SIGMON,[27] to yield $\sigma_{1j} = 3.79$ Å and $\epsilon_{1j} = 354$ K for monothioformic acid and $\sigma_{1j} = 3.96$ Å and $\epsilon_{1j} = 378$K for dithioformic acid. A weak-collision "exponential down" model for energy transfer between reactants and Ar was assumed. The remaining molecular properties were taken from the MP2/6-311G** calculations. We used the UNIMOL program[28] to calculate the high-pressure rate constant of the reactions in Arrhenius form as a function of temperature. Clearly, the reaction rate constant is too small to be measured at room temperature. In the range of 700−2000 K, the variation of rate k_1 for dehydrogensulfidation channel and k_2 for dehydrogenation channel of *keto*-HC(:O)SH can be represented as $k_1 = 1.38 \times 10^{10} \exp(-23840/T)$ s^{-1} and $k_2 = 2.96 \times 10^{10} \exp(-27320/T)$ s^{-1}, respectively. The *A*-factors in k_1 and k_2 are of the same order. The exponential factor of k_2 is much smaller than that of k_1, which means the activation energy in reaction 2 is much higher than that in reaction 1; we obtain $k_1 > k_2$ at any temperature in our calculations. Similarly, the variation of rate k_3 for the dehydration channel and k_4 for the dehydrogenation channel of *thioketo*-HC(:S)OH can be represented as $k_3 = 1.84 \times 10^{11} \exp(-37590/T)$ s^{-1} and $k_4 = 3.47 \times 10^{10} \exp(-28520/T)$ s^{-1}, respectively, and we can find $k_4 > k_3$; the variation of rate k_5 for reaction 5 and k_6 for reaction 6 can be described by $k_5 = 1.74 \times 10^{10} \exp(-24280/T)$ s^{-1} and $k_6 = 6.07 \times 10^{10} \exp(-30600/T)$ s^{-1}, respectively, and we obtain $k_5 > k_6$.

Conclusion

Calculations both at the SCF level and at the MP2 level, including electron correlation effects on both the geometries and energies of the different stationary points encountered along the decomposition pathways, for thioformic acids, have been reported. All of the *trans* isomers are slightly more stable than the corresponding *cis* isomers. Moreover, for monothioformic acid, the *keto* conformer is more stable than the *thioketo* conformer. Three pairs of competing pyrolysis reactions have been examined and discussed in terms of ab initio and RRKM calculations. From the calculations we obtain $k_1 > k_2$, $k_4 > k_3$, and $k_5 > k_6$.

Appendix

The total energies (hartrees) at different levels of the stationary points for thioformic acid decomposition are given in Table 3.

References and Notes

(1) Strorer, A. C.; Murphy, W. F.; Carey, P. R. *J. Biol. Chem.* **1979**, *254*, 3163.
(2) Hocking, W. H.; Winnewisser, G. *J. Chem. Soc., Chem. Commun.* **1975**, *2*, 63.
(3) Engler, R.; Gattow, G. *Z. Anorg. Allg. Chem.* **1972**, *78*, 388.
(4) Hocking, W. H.; Winnewisser, G. *Z. Naturforsch., A* **1976**, *31*, 422.
(5) Bak, B.; Nielsen, O. J.; Svanholt, H. *J. Mol. Spectrosc.* **1978**, *69*, 401.
(6) Bak, B.; Nielsen, O. J.; Svanholt, H. *J. Mol. Spectrosc.* **1975**, *75*, 134.
(7) Fausto, F.; Teixiera-Dias, J. J. C.; Carey, P. R. *THEOCHEM* **1978**, *37*, 119.
(8) So, S. P. *J. Mol. Struct.* **1986**, *148*, 153.
(9) So, S. P. *THEOCHEM* **1986**, *33*, 153.
(10) Ioannoni, F.; Moule, D. C.; Goddard, J. P.; Cleuther, D. J. *J. Mol. Struct.* **1989**, *197*, 159.
(11) Fausto, R.; Teixiera-Dias, J. J. C.; Carey, P. R. *J. Mol. Struct.* **1989**, *212*, 61.
(12) Fausto, R.; Teixiera-Dias, J. J. C.; Carey, P. R. *J. Mol. Struct. (THEOCHEM)* **1988**, *168*, 179.
(13) Tao, Y. Q. *Chem. Phys.* **1991**, *154*, 221.
(14) Nguyen, M. T.; Weringa, W. D. *J. Phys. Chem.* **1989**, *93*, 7956.
(15) Fausto, R. *J. Mol. Struct. (THEOCHEM)* **1994**, *351*, 123.
(16) Xie, X. G.; Tao, Y. Q.; Cao, H.; Duang, W. G. *Chem. Phys.* **1996**, *213*, 133.
(17) Ruelle, P.; Kesselring, U. W.; Nam-Tran, H. *J. Am. Chem. Soc.* **1986**, *108*, 371.
(18) Császár, A. G. *J. Phys. Chem.* **1996**, *100*, 3541.
(19) Frisch, M. J.; Trucks, G. W.; Head-Gordon, M.; Gill, P. M. W.; Wong, M. W.; Foresman, J. B.; Johnson, B. G.; Schlegel, H. B.; Robb, M. A.; Reglogle, E. S.; Gomperts, T.; Andres, J. L.; Raghavachari, K.; Binkley, J. S.; Gonzales, C.; Martin, R. L.; Fox, D. J.; DeFrees, D. J.; Baker, J.; Stewart, J. J. P.; Pople, J. A. *GAUSSIAN 94W* (Revision A); Gaussian, Inc.: Pittsburgh, PA, 1994.
(20) Møller, C.; Plesset, M. S. *Phys. Rev.* **1934**, *46*, 618.
(21) Pople, J. A.; Binkley, J. S.; Seeger, R. *Int. J. Quantum Chem. Symp.* **1979**, *10*, 1.

(22) Schmidt, M. W.; Gordon, M. S.; Dupuis, M. *J. Am. Chem. Soc.* **1985**, *107*, 2585, and references cited therein.
(23) DeFrees, D. J.; Levy, B. A.; Pollack, S. K.; Hehre, W. J.; Binkley, J. S.; Pople, J. A. *J. Am. Chem. Soc.* **1979**, *101*, 4085.
(24) Gilbert, R. G.; Smith, S. C. *Theory of Unimolecular and Recombination Reactions*; Blackwell: Oxford, U.K., 1990.
(25) Gilbert, R. G.; Luther, L.; Troe, J. *J. Ber. Bunsen-Ges. Phys. Chem.* **1983**, *87*, 169.
(26) Smith, S. C.; Mceman, M. J.; Gilbert, R. G. *J. Chem. Phys.* **1989**, *90*, 4265.
(27) Lim, K. F. Program SIGMON: An aid for the semiempirical fitting of the intermolecular potential, available from K. F. Lim, School of Chemistry, University of Melbourne, Parkville, VIC 3052, Australia, 1992.
(28) Gilbert, R. G.; Jordan, M. J. T.; Smith, S. C. UNIMOL programs suite (calculation of fall-off curves for unimolecular and recombination reactions), 1993.